



# Inversion of the acetabular labrum causes increased localized contact pressure on the femoral head: a biomechanical study

Xipeng Wang<sup>1</sup> · Kiyokazu Fukui<sup>2</sup> · Ayumi Kaneuji<sup>2</sup> · Kenichi Hirotsaki<sup>3</sup> · Hiroyasu Miyakawa<sup>3</sup> · Norio Kawahara<sup>2</sup>

Received: 28 June 2018 / Accepted: 3 December 2018 / Published online: 11 December 2018  
© SICOT aisbl 2018

## Abstract

**Purpose** Although studies suggest that subchondral insufficiency fracture of the femoral head may cause rapidly progressive osteoarthritis of the hip, the mechanism of that relationship remains unclear. Our biomechanical study aimed to provide more data in this area by quantifying pressure distribution on the femoral head for normal and inverted hips and by determining the effects of labral inversion on pressure distribution across the joint, focusing on types of fracture under load.

**Methods** We tested mid-sized fourth-generation composite femurs at 15° of adduction, and applied 1 mm/min of axial compressive force to the femoral heads until failure. Additionally, single loads (3000 N) were applied using Prescale film to investigate pressure distribution on the femoral head, with or without silicone rubber representing entrapment of an inverted acetabular labrum.

**Results** In tests with an external load of 3000 N, the mean pressure for 10 × 5 mm of silicone rubber was 11.09 MPa, significantly greater (about 5.7-fold) than 1.94 MPa without silicone rubber. Different fracture patterns were observed with and without the 10 × 5 mm silicone rubber; when the 10 × 5 mm silicone rubber specimens were used, all eight cases showed fractures in the anterior femoral head.

**Conclusions** When silicone rubber representing an inverted acetabular labrum was placed between a hemispherical metallic platen and a composite bone model, the silicone rubber areas were subjected to extreme concentration of stress. The fractures that developed at the silicone rubber areas clearly represented subchondral fractures of the femoral head, rather than fractures of the femoral neck.

**Keywords** Inverted acetabular labrum · Subchondral fracture of the femoral head · Rapidly progressive osteoarthritis of the hip · Contact pressure · Biomechanical study

## Introduction

Although subchondral stress fractures of the femoral head do not occur widely in general [1–4], subchondral insufficiency-

type stress fracture (SIF) of the femoral head is recognized as a predominant aetiology of rapidly progressive osteoarthritis of the hip joint. A recent study also reports SIF of the femoral head occurring in military recruits and in patients with tumour-induced osteomalacia [5, 6]. Rapidly progressive osteoarthritis (OA) of the hip, also known as rapidly destructive osteoarthritis of the hip, is a rare condition that can destroy the joint, usually within a period of six months to three years. First reported by Postel and Kerboul in 1970 [7], the disease was defined by Lequesne as chondrolysis >2 mm in one year, or 50% joint space narrowing in one year [8], with no evidence of other forms of rapidly destructive arthropathy such as osteonecrosis or Charcot neuroarthropathy. The disease is particularly prevalent in elderly female patients and can be both painful and disabling. It is becoming more common as the population ages and is associated with an increased incidence of total hip arthroplasty (THA) [9]. However, little information is available

---

✉ Kiyokazu Fukui  
66406kf@kanazawa-med.ac.jp

<sup>1</sup> Department of Orthopedic Surgery, Liyuan Hospital, Tongji Medical College, Huazhong University of Science and Technology, Wuhan, Hubei 430007, China

<sup>2</sup> Department of Orthopedic Surgery, Kanazawa Medical University, 1-1 Daigaku, Uchinada-machi, Kahoku-gun, Ishikawa 920-0293, Japan

<sup>3</sup> Department of Machinery and Metal, Industrial Research Institute of Ishikawa, 2-1, Kuratsuki, Kanazawa, Ishikawa 920-8203, Japan

on the etiology of SIF, and this lack of information interferes with efforts toward early diagnosis and treatment.

Some studies suggest that SIF of the femoral head may encourage rapidly progressive OA of the hip [10–16]. However, most insufficiency fractures occur as femoral neck fractures at the proximal femur during loading of the joint [17–19]; why do some occur instead in the subchondral area of the femoral head? Most recently, Fukui et al. proposed that inversion of the acetabular labrum may be involved in subchondral insufficiency fracture with subsequent rapidly destructive hip OA [20–22]. They reported that inversion of the anterosuperior portion of the labrum was confirmed intra-operatively in nine patients with early-stage rapidly destructive hip OA. In addition, eight of the nine patients showed SIF in the anterosuperior portion of the femoral heads beneath the inverted region of the labrum. However, questions remain regarding whether an inverted labrum causes SIF directly or contributes to the mechanism for this progression.

The purpose of this study was to quantify pressure distribution on the acetabular rim for normal and inverted hips to determine how labral inversion changes the pressure distribution across the joint. We hypothesized that inversion of the acetabular labrum causes an increase in localized pressure, both on the anterosuperior region of the acetabulum and on the femoral head just under the inverted labrum.

## Materials and methods

### Specimen preparation

We used mid-size fourth-generation composite femurs with a solid cancellous bone density of  $0.13 \text{ g/cm}^3$  (Sawbones, Pacific Research Laboratories, Inc., Vashon, WA). Previous research has shown that composite femurs resemble cadaveric femurs in failure mode, stiffness, and strength, but without the anatomic variability found in cadaveric bone [23, 24]. The composite femurs were cut 100 mm distal to the inferior margin of the lesser trochanter, leaving a total length of 200 mm. The distal-most 100 mm of each femur was then potted in epoxy resin (crystal resin Neo Nissin Resin Co., Ltd., Kanagawa, Japan) in a cylindrical mold; the long axis of the femur was aligned with the cylindrical axis of the mold. The working length of the femur from the top of the femoral head to the shaft insertion in the epoxy resin was thus 100 mm (Fig. 1a). We made a hemispherical metallic platen molded to the shape of the composite femoral head and attached it to a load actuator. The platen was made from carbon steel S45C with a smooth surface finish to minimize friction (Fig 1b). To represent an inverted acetabular labrum, we chose silicone rubber that possessed material properties similar to the labrum in compressive stiffness (G3548LN, Du Pont-Toray Co., Ltd., Tokyo, Japan) [25]. This silicone rubber had a thickness of 4 mm. For our experiments, we cut samples  $10 \times 5 \text{ mm}$  and

**Fig. 1** The biomechanical test set-up (a) with the spherical metal platen (b) in the tensile testing machine. The silicone rubber, 4 mm thick, was cut into  $10 \times 5 \text{ mm}$  and  $10 \times 20 \text{ mm}$  pieces and used to represent an inverted acetabular labrum (c)

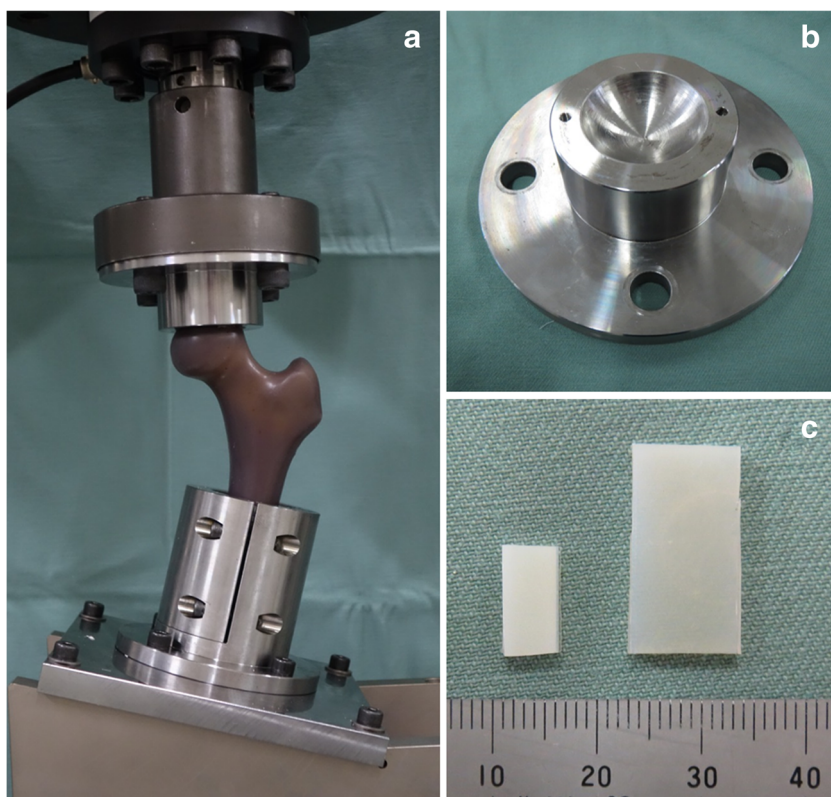
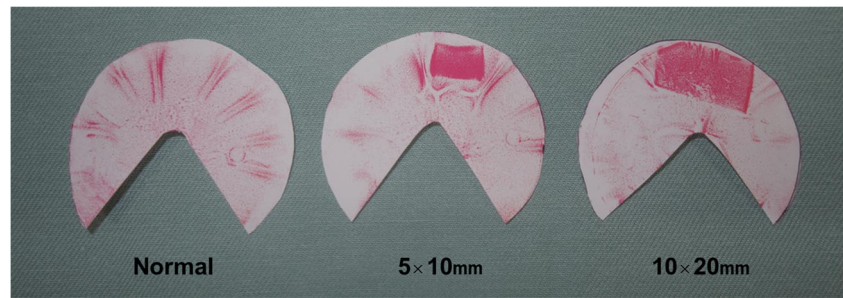


**Fig. 2** A load of 3000 N, as measured by ordinary Prescale film, was applied to specimens in each group. Deeper pink colour indicates higher contact pressure. The silicone rubber area in the 10 × 5 mm group showed the deepest color



10 × 20 mm in size and placed them between a hemispherical metal platen and the anterior surface of the head of the composite femur (Fig. 1c).

### Biomechanical testing

Specimens were fixed in a tensile testing machine (EHF-UM 300KN-70L; Shimadzu Corp., Kyoto, Japan) with a custom steel jig and were aligned to 15° of adduction in the coronal plane, as previously reported [26]. For each specimen, we applied a compressive pre-load of 10 N with the flat or conical platen to the femoral head and maintained that pre-load for ten seconds to establish the time-zero position. We then loaded the specimens to failure at a displacement-controlled rate of 1 mm/min and observed fracture patterns [27]. To record load and position data, we used a testing system software (Shimadzu Gluon ver.2.50C, Kyoto, Japan). Ultimate failure load was identified, and stiffness and energy to failure were calculated. We tested 16 composite femurs in total, consisting of two groups, eight composite femurs without silicone rubber

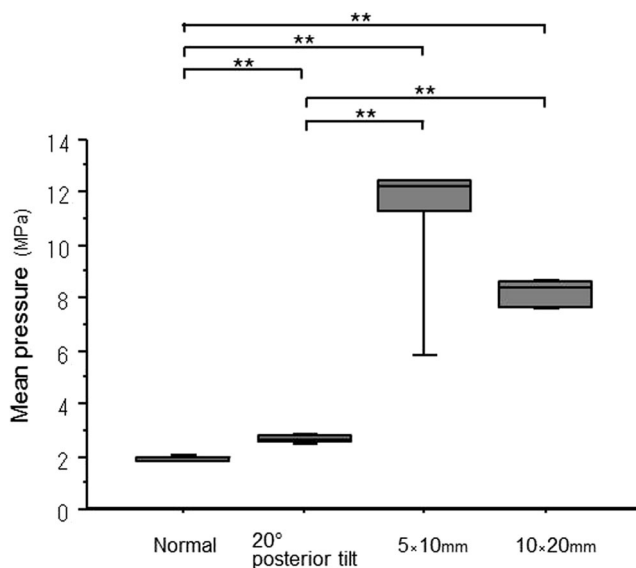


**Fig. 3** Box plots of mean pressure for the normal group ( $n = 6$ ), 10 × 5 mm group ( $n = 6$ ), and 10 × 20 mm group ( $n = 6$ ). The horizontal line indicates the median. The box extends from the 25th to the 75th percentile, and the bars indicate the largest and smallest observed values. An asterisk represents significant difference ( $p < 0.01$ )

and 8 with 10 × 5 mm silicone rubber. Room temperature was maintained at 20 °C.

A specially prepared pre-cut Fujifilm product (Prescale, Fujifilm Corp., Tokyo, Japan) was used to assess contact stress on the composite femoral head. First, a single load (3000 N) was applied. The test load of 3000 N was considered to be equivalent to the hip joint load for a 70-kg person standing on one leg. Each piece of the Prescale film was pre-cut in the shape of a circle with a wedge removed (“Pac-Man” shape) and placed it on the surface of the composite femoral head with care for avoiding wrinkling. Peak pressures were determined from the colour density of the Prescale film, using a Prescale Pressure Image Analysis System FPD-8010J (Fujifilm Corp., Tokyo, Japan) operated by two orthopaedic surgeons (XW and KF) with more than eight years of clinical experience each. Measurements were performed three times for each sample of the Fujifilm, and mean values were calculated. Six tests were performed in each of the three groups (normal group, no silicone rubber; 10 × 5 mm group, 10 × 5 mm silicone rubber between the spherical metallic platen and the femoral head of the composite bone; 10 × 20 mm group, 10 × 20 mm silicone rubber between the platen and the femoral head). We measured mean pressure on the area of silicone rubber in the 10 × 5 mm and 10 × 20 mm specimens. In the normal specimens, we measured mean pressure on the anterior portion of the spherical metallic platen over almost the same area as was covered by silicone rubber in the 10 × 5 mm and 10 × 20 mm specimens. Overall, inter-observer reliability of those measurements between the two surgeons was high (intra-class coefficient 0.84, 95% confidence interval (CI) 0.72–0.92). All disagreements were resolved by simultaneous re-reading and consensus opinion.

### Finite element analysis

A three-dimensional computer-aided design (CAD) model of a mid-size left fourth-generation composite femur (Model 3403, Sawbones, Vashon, WA, USA) was employed. The CAD model was imported into the ANSYS Workbench (ANSYS Inc., Canonsburg, PA, USA) to generate an FE model with 312,933 nodes and 208,377 elements for static structural analysis (Fig. 5a). The cortical bone had a Young’s modulus of 16.35 GPa and Poisson’s ratio of 0.26. The cancellous

**Table 1** Contact pressure on the anterior portion of the femoral head

	Normal	20° posterior tilt	5 × 10 mm	10 × 20 mm
Mean pressure (SD) (MPa)	1.94 (0.09)	2.65 (0.15)	11.09 (2.47)	8.22 (0.47)
Mean maximum pressure (SD) (MPa)	6.74 (0.60)	8.88 (0.68)	12.75 (0)	12.75 (0)
Mean measured area (SD) (mm <sup>2</sup> )	172 (33)	159 (28)	77 (14)	217 (29)

bone had a Young's modulus of 0.137 GPa and Poisson's ratio of 0.3.

The composite femurs were analyzed from the apex of the femoral head at a 15° tilt to a horizontal line 12 mm below the apex. The following three loading regions were designated for the ultimate failure load test: the "normal region" in specimens with no silicone rubber, the "10 × 5 mm region" in specimens with 10 × 5 mm silicone rubber, and the "10 × 20 mm region" in specimens with 10 × 20 mm silicone rubber. In the normal region, the load vector was oriented vertically, and the load was distributed uniformly throughout the region. In the 10 × 5 mm region and the 10 × 20 mm region, a plane of projection was set to be a rectangle having an aspect ratio of 1:2 around the point 5 mm anterior to the apex of the femoral head at a 15° tilt. The load vector was oriented vertically toward the center of the region and was distributed throughout the region (Fig. 5b).

### Statistical analysis

Statistical analysis was performed with the use of a predictive analytics software (SPSS Statistics version 21; IBM, Armonk, NY, USA). The study compared data for each group using an independent *t* test. Statistical significance was set at  $P < 0.05$ .

## Results

### Pressure distribution on the femoral head

In tests using a load of 3000 N, we found that the presence or absence of silicone rubber resulted in considerable difference in stress values and stress distribution on the surface of the

femoral head (Figs. 2 and 3). In the presence of the 10 × 5 mm silicone rubber, mean pressure was 11.09 MPa, approximately 5.7-fold higher than in the absence of the silicone rubber in the normal samples (1.94 MPa). This difference was statistically significant ( $P < 0.0001$ ). Findings were similar in the 10 × 20 mm samples, with pressure approximately 4.2-fold higher than in the normal samples. To produce a model of posterior pelvic tilt, the hemispherical metallic platen was shifted 20° posterior. Findings were then compared for the presence and absence of this posterior tilt. Pressure of the anterior portion of the femoral head was significantly higher in the presence of the posterior tilt, but the increase in pressure did not exceed 1.3-fold that of the normal samples (Table 1).

### Fracture pattern and ultimate failure load, stiffness

#### Fracture pattern

Different fracture patterns were observed in the presence or absence of 5 × 10 mm silicone rubber (Fig. 4).

In all eight specimens without silicone rubber, fractures occurred in the posterior femoral neck. However, fractures occurred in the anterior femoral head in all eight specimens with 10 × 5 mm silicone rubber.

#### Ultimate failure load, stiffness, and energy

Load application in specimens with 10 × 5 mm silicone rubber yielded the following results (mean ± SD): ultimate failure load 8977 ± 1520 N, stiffness 3600 ± 326 N/mm, and energy to failure 14.78 ± 3.43 J. Those three parameters in the 10 × 5 mm group did not differ significantly from the group

**Fig. 4** Commonly observed fracture patterns associated with no silicone rubber (a) and 10 × 5 mm silicone rubber (b)

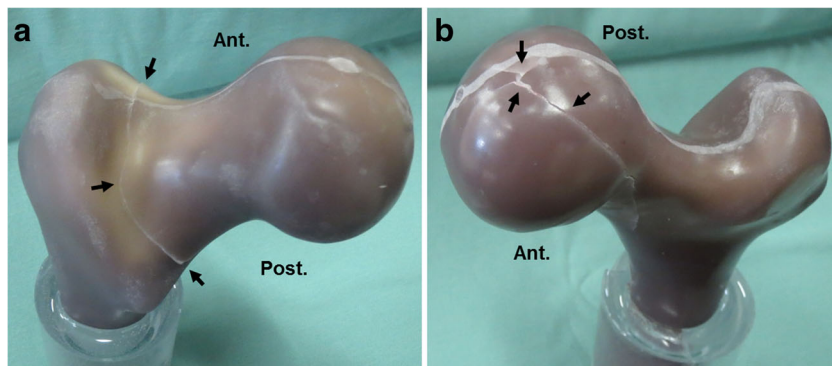




**Table 2** Differences in maximum principal stress by applying a 3000 N load

Loading area	Maximum principal stress (MPa)		
	Region a 15° 3000 N	Region b	Region c
Normal	57.8	33.5	-0.1
5 × 10 mm	37.8	31.6	85.8
10 × 20 mm	37.8	32.2	25.1

without silicone rubber ( $8540 \pm 1108$  N,  $3154 \pm 626$  N/mm, and  $14.75 \pm 2.91$  J, respectively).

### Finite element analysis

When we applied a load of 3000 N to normal regions, maximum principal stress developed mainly at the posterior femoral neck (region a). However, in the  $10 \times 5$  mm regions, maximum principal stress developed mainly at the subchondral area of the femoral head (region c) (Table 2). These results emphasize the differences in fracture pattern in the ultimate failure load test. We also recorded the distribution of maximum principal stress when load was applied to the  $10 \times 5$  mm region (Fig. 5c).

### Discussion

Fukui et al. noted inversion of the acetabular labrum in initial-stage rapidly destructive hip OA and proposed that this inversion may relate to SIF of the femoral head due to the concentration of stress on the subchondral bone. (Fig. 6). To the best of our knowledge, there have been no reports of stress distribution associated with labral entrapment between the femoral head and the acetabulum. This research elucidates the major changes in stress distribution on the femoral head surface due

to entrapment within the joint, such as by an inverted acetabular labrum. SIF of the femoral head is considered to be one possible mechanism for the onset of rapidly progressive osteoarthritis of the hip, but the process by which this occurs is not well-characterized. If fragility is the only cause, we would expect fractures at the femoral neck rather than at the femoral head beneath the cartilage [28].

The acetabular labrum consists of a ring of fibrocartilage that functions as a “suction seal” to ensure continuous lubrication of the hip joint. Some researchers suggest that the labrum maintains negative intra-articular pressure within the hip joint, which enhances stability; in a normal gait, the labrum may also prevent joint expansion and improve kinematics by acting as a tension band. Further improvements in joint stability and kinematics are achieved by distributing the force of contact and creating a functionally deeper hip joint [29–32].

When the suction seal operates effectively, stress will be applied at the surface of the femoral head and will be distributed uniformly within the central compartment in accordance with Pascal’s principle. As the anterior coverage decreases on the femoral head, this reduces the load-bearing area of the femoral head where normal stress is placed. For the same amount of weight-bearing, we can thus hypothesize that the stress within the central compartment would increase, assuming that the stress is distributed uniformly across the load-bearing area of the femoral head.

Some researchers [33] have suggested that posterior pelvic tilt may contribute to SIF. However, our research suggests that a 20° posterior pelvic tilt is associated with a mean stress value approximately 1.3-fold higher than normal. From this, we can infer that subchondral fracture of the femoral head due to posterior pelvic tilt would require a substantial weight-bearing load as well as considerable fragility in the femoral head.

When Nicayenzi et al. used fourth-generation composite femurs at 15° tilt and compressed the femoral heads with a spherical stainless steel cup at a rate of 5 mm/min, the average ultimate failure load for specimens with a cancellous density

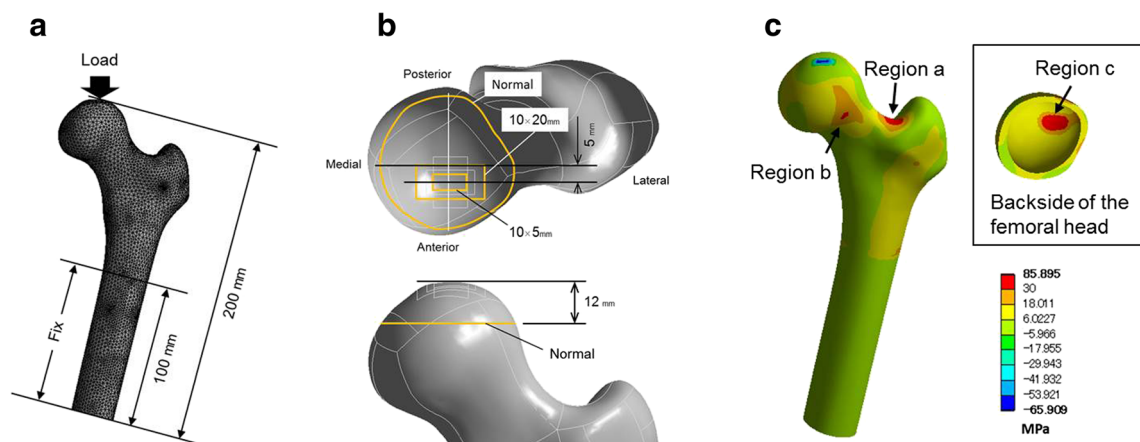
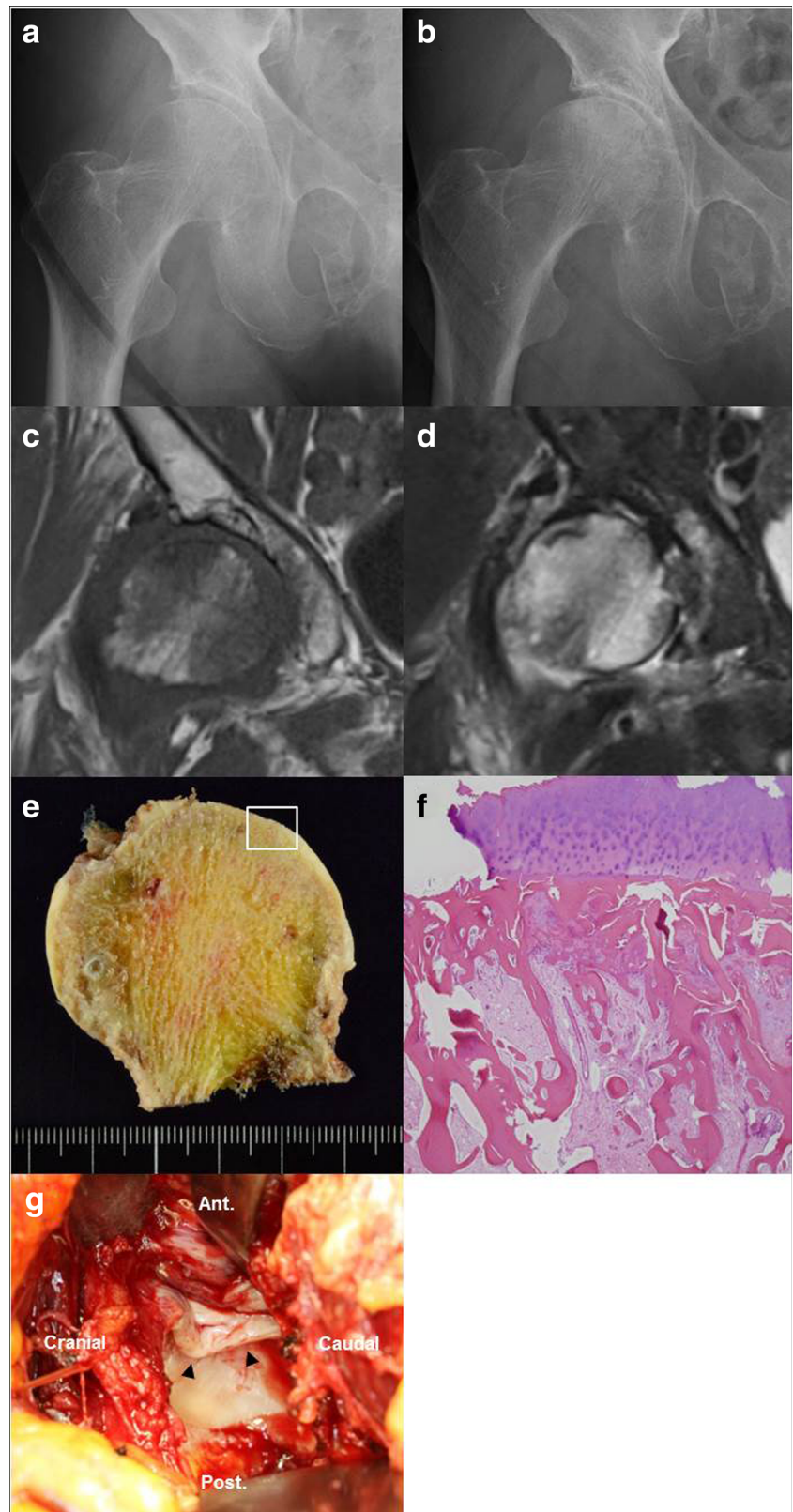


**Fig. 5** Exploded view of a finite element model of the composite femur (a). Diagram showing the three different areas of loading 3000 N (b). A typical graph of the maximum principal stress in the bone at the  $10 \times 5$  mm loading area (c)

**Fig. 6** A 74-year-old woman who had initial-stage rapidly progressive osteoarthritis of the right hip. An AP radiograph showed rapid narrowing of the joint space in just 3 months (**a, b**). One month after the onset of right hip pain, magnetic resonance images showed bone marrow oedema from the upper portion of the femoral head (T1-weighted image with diffuse low-intensity signal (**c**), short  $\tau$  inversion recovery (STIR) sequence with high-intensity signal (**d**)). A whitish-gray zone was noted beneath the lateral articular cartilage (box) in the mid-coronal cut section of the resected femoral head (**e**). Under haematoxylin and eosin stain, histopathology of the resected femoral head showed an accumulation of fracture callus and granulation tissue around the subchondral fractured lesion within the white rectangle in **e** (**f**). There was unmistakable inversion of the labrum at the anterosuperior portion (**arrowheads**) (**g**)



of  $0.16 \text{ g/cm}^3$  was 7092 N. These specimens reportedly failed due to transcervical fracture of the femoral neck, much like the specimens without silicone rubber in the present study [34].

In our simulation using  $10 \times 5 \text{ mm}$  silicone rubber, the amount of stress through the anterior femoral head of our bone model increased by approximately 5.7-fold. This stress was

higher than with the 10 × 20 mm silicone rubber. The area of high-pressure contact between the platen and the femoral head in the 10 × 5 mm silicone rubber group (mean 77 mm<sup>2</sup>) was smaller than in the 10 × 20 mm silicone rubber group (mean 217 mm<sup>2</sup>); stress was concentrated on a smaller area and resulted in higher pressure per unit area in the 10 × 5 mm group.

With no silicone rubber, we saw fractures of the femoral neck. However, with the silicone rubber, we observed depression and split fractures of the femoral head. This suggests that presence of an inverted acetabular labrum could be an important factor in the development of subchondral fractures. These results also seem to indicate that the inverted area of the labrum is smaller, which increases the likelihood of subchondral fractures due to stress concentration on the femoral head.

We hypothesized that load application in the silicone rubber specimens would result in significantly lower ultimate failure load, stiffness, and energy to failure than in the specimens without silicone rubber. However, we actually found no significant difference in ultimate failure load between 10 × 5 mm silicone rubber and normal specimens. This may have been due to subtle differences in specimen position setting and material properties in the individual composite femurs.

We note several limitations of the current study. First, the cancellous bone density of the femur specimens in this study was 0.13 g/cm<sup>3</sup>, considerably lower than the standard cancellous bone density of 0.27 g/cm<sup>3</sup> that is used in fourth-generation composite femurs [35]. However, low bone densities are common in patients with SIF of the femoral head, and osteoporotic bone models are not yet commercially available, so we considered it appropriate to use a composite bone model with a lower cancellous density. We feel that this position is supported by Basso et al., who suggested that until a validated osteoporotic composite femur model is provided, standard fourth-generation composite femurs should only be used when representing the biomechanical properties of young healthy femurs [36].

Second, fracture patterns are not yet fully characterized, and further investigation using cadaveric femurs or osteoporotic composite femur models is needed. However, in the current study, the remarkable difference in fracture pattern with and without silicone rubber between the composite femoral head and hemispherical metal platen indicated that an intra-articular inclusion such as an inverted acetabular labrum could play an important role in the pathomechanism of SIF of the femoral head. Third, the short working length of the femurs (100 mm) in the current study prevented the physiologic load distribution that occurs in full-length femurs, which may have enhanced the observed differences.

In addition, this study involved only a single load-bearing experiment. However, in reality, subchondral fractures in the femoral head may occur as a consequence of repeated load-bearing events. Further research is required to determine

whether the same results will be obtained from repeated load-bearing tests.

Finally, the hemispherical platen produced more physiologic loading than the flat platen but was not an accurate representation of the acetabulum anatomy.

In conclusion, this research showed that, when silicone rubber resembling the inverted labrum was placed between a hemispherical metallic platen and a composite bone model, the areas where the silicone rubber was present were subjected to extreme concentration of stress. In addition, this stress concentration at the silicone rubber areas was clearly characterized as the equivalent of subchondral fractures of the femoral head, rather than fractures of the femoral neck. Our results confirm the hypothesis that inversion of the acetabular labrum contributes to subchondral stress fracture, and suggest that such inversion also plays a major role in the development of subchondral insufficiency fractures. Such fractures, in turn, contribute greatly to the pathomechanism of rapidly progressive hip osteoarthritis, which has seen a sharp increase in recent years. Although the cause of inversion of the labrum is still unclear, several conditions such as posterior pelvic tilt, femoroacetabular impingement, or extra-articular hip impingement may be involved in entrapment of the labrum [21, 37]. Further investigation is needed to find the correlation between the inversion of the labrum and morphological features. If procedures can be devised for the early detection and treatment of inversion of the acetabular labrum, it may be possible to prevent rapidly progressive hip OA.

**Acknowledgments** We thank Lee Seaman of Seaman Medical, Inc. (Bellingham, WA, USA) for providing the professional English-language editing of this article.

**Funding** This research did not receive any specific grants from funding agencies in the public, commercial, or not-for-profit sectors.

## Compliance with ethical standards

**Conflict of interest** The authors declare that they have no conflict of interest.

**Ethical approval** This article does not contain any studies with human participants or animals performed by any of the authors.

## References

1. Kim SM, Oh SM, Cho CH, Lim SJ, Moon YW, Choi SH, Park YS (2016) Fate of subchondral fatigue fractures of femoral head in young adults differs from general outcome of fracture healing. *Injury* 47:2789–2794. <https://doi.org/10.1016/j.injury.2016.10.014>
2. Buttaro M, Della Valle AG, Morandi A, Sabas M, Pietrani M, Piccaluga F (2003) Insufficiency subchondral fracture of the femoral head: report of 4 cases and review of the literature. *J Arthroplast* 18:377–382. <https://doi.org/10.1054/arth.2003.50092>



3. Yamamoto T, Nakashima Y, Shuto T, Jingushi S, Iwamoto Y (2007) Subchondral insufficiency fracture of the femoral head in younger adults. *Skelet Radiol* 36:S38–S42. <https://doi.org/10.1007/s00256-006-0178-1>
4. Motomura G, Yamamoto T, Miyaniishi K, Shirasawa K, Noguchi Y, Iwamoto Y (2002) Subchondral insufficiency fracture of the femoral head and acetabulum: a case report. *J Bone Joint Surg Am* 84:1205–1209
5. Song WS, Yoo JJ, Koo KH, Yoon KS, Kim YM, Kim HJ (2004) Subchondral fatigue fracture of the femoral head in military recruits. *J Bone Joint Surg Am* 86:1917–1924
6. Kobayashi H, Ito N, Akiyama T, Okuma T, Kinoshita Y, Ikegami M, Shinoda Y, Fukumoto S, Tanaka S, Kawano H (2017) Prevalence and clinical outcomes of hip fractures and subchondral insufficiency fractures of the femoral head in patients with tumour-induced osteomalacia. *Int Orthop* 41(12):2597–2603. <https://doi.org/10.1007/s00264-017-3610-3>
7. Postel M, Kerboul M (1970) Total prosthetic replacement in rapidly destructive arthrosis of the hip joint. *Clin Orthop Relat Res* (72):138–144
8. Lequesne M (1970) Rapid destructive coxarthrosis. *Rhumatologie* 22:51–63
9. Flemming DJ, Gustas-French CN (2017) Rapidly progressive osteoarthritis: a review of the clinical and radiologic presentation. *Curr Rheumatol Rep* 19(42). <https://doi.org/10.1007/s11926-017-0665-5>
10. Bangil M, Soubrier M, Dubost JJ, Rami S, Carcanagus Y, Ristori J, Burriere J (1996) Subchondral insufficiency fracture of the femoral head. *Rev Rhum Engl Ed* 63:859–861. [https://doi.org/10.1002/1529-0131\(199912\)42:12](https://doi.org/10.1002/1529-0131(199912)42:12)
11. Yamamoto T, Bullough PG (1999) Subchondral insufficiency fracture of the femoral head: a differential diagnosis in acute onset of coxarthrosis in the elderly. *Arthritis Rheum* 42:2719–2723. [https://doi.org/10.1002/1529-0131\(199912\)42:12<2719::AID-ANR31>3.0.CO;2-X](https://doi.org/10.1002/1529-0131(199912)42:12<2719::AID-ANR31>3.0.CO;2-X)
12. Hagino H, Okano T, Teshima R, Nishi T, Yamamoto K (1999) Insufficiency fracture of the femoral head in patients with severe osteoporosis: report of 2 cases. *Acta Orthop Scand* 70:87–89
13. Rafii M, Mitnick H, Klug J, Firooznia H (1997) Insufficiency fracture of the femoral head: MR imaging in three patients. *AJR* 168:159–163
14. Yamamoto T, Bullough PG (2000) The role of subchondral insufficiency fracture in rapid destruction of the hip joint. *Arthritis Rheum* 43:2423–2427. [https://doi.org/10.1002/1529-0131\(200011\)43:11<2423::AID-ANR8>3.0.CO;2-Z](https://doi.org/10.1002/1529-0131(200011)43:11<2423::AID-ANR8>3.0.CO;2-Z)
15. Yamamoto T, Takabatake K, Iwamoto Y (2002) Subchondral insufficiency fracture of the femoral head resulting in rapid destruction of the hip joint: a sequential radiographic study. *AJR Am J Roentgenol* 178:435–437
16. Watanabe W, Itoi E, Yamada S (2002) Early MRI findings of rapidly destructive coxarthrosis. *Skelet Radiol* 31:35–38. <https://doi.org/10.1007/s00256-001-0445-0>
17. Davies AM, Bradley SA (1991) Iliac insufficiency fractures. *Br J Radiol* 64:305–309. <https://doi.org/10.1259/0007-1285-64-760-305>
18. Lin J, Lachmann E, Nagler W (2001) Sacral insufficiency fractures: a report of two cases and a review of the literature. *J Womens Health Gend Based Med* 10:699–705. <https://doi.org/10.1089/15246090152563588>
19. Verhaegen MJ, Sauter AJ (1999) Insufficiency fractures, an often unrecognized diagnosis. *Arch Orthop Trauma Surg* 119:115–116
20. Fukui K, Kaneuji A, Fukushima M, Matsumoto T (2014) Inversion of the acetabular labrum triggers rapidly destructive osteoarthritis of the hip: representative case report and proposed etiology. *J Arthroplast* 29:2468–2472. <https://doi.org/10.1016/j.arth.2014.06.017>
21. Fukui K, Kaneuji A, Fukushima M, Matsumoto T (2015) Early MRI and intraoperative findings in rapidly destructive osteoarthritis of the hip: a case report. *Int J Surg Case Rep* 8:13–17. <https://doi.org/10.1016/j.ijscr.2015.01.009>
22. Fukui K, Kaneuji A, Fukushima M, Matsumoto T (2014) Imaging and histopathological evaluation of a cystlike formation in subchondral insufficiency fracture of the femoral head: a case report and literature review. *Int J Surg Case Rep* 5:324–329. <https://doi.org/10.1016/j.ijscr.2014.03.024>
23. Gardner MP, Chong AC, Pollock AG, Wooley PH (2010) Mechanical evaluation of large-size fourth-generation composite femur and tibia models. *Ann Biomed Eng* 38:613–620. <https://doi.org/10.1007/s10439-009-9887-7>
24. Heiner AD (2008) Structural properties of fourth-generation composite femurs and tibias. *J Biomech* 41:3282–3284. <https://doi.org/10.1016/j.jbiomech.2008.08.013>
25. Smith CD, Masouros S, Hill AM, Amis AA, Bull AM (2009) A biomechanical basis for tears of the human acetabular labrum. *Br J Sports Med* 43:574–578. <https://doi.org/10.1136/bjsm.2008.053645>
26. Takahashi E, Kaneuji A, Tsuda R, Numata Y, Ichiseki T, Fukui K, Kawahara N (2017) The influence of cement thickness on stem subsidence and cement creep in a collarless polished tapered stem: when are thick cement mantles detrimental? *Bone Joint Res* 6:351–357. <https://doi.org/10.1302/2046-3758.65.BJR-2017-0028.R1>
27. Wijdicks CA, Balldin BC, Jansson KS, Stull JD, LaPrade RF, Philippon MJ (2013) Cam lesion femoral osteoplasty: in vitro biomechanical evaluation of iatrogenic femoral cortical notching and risk of neck fracture. *Arthroscopy* 29:1608–1614. <https://doi.org/10.1016/j.arthro.2013.06.021>
28. Yoshikawa T, Turner CH, Peacock M et al (1994) Geometric structure of the femoral neck measured using dual-energy x-ray absorptiometry. *J Bone Miner Res* 9:1053–1064. <https://doi.org/10.1002/jbmr.5650090713>
29. Crawford MJ, Dy CJ, Alexander JW et al (2007) The 2007 Frank Stinchfield Award. The biomechanics of the hip labrum and the stability of the hip. *Clin Orthop Relat Res* 465:16–22
30. Ferguson SJ, Bryant JT, Ganz R, Ito K (2003) An in vitro investigation of the acetabular labral seal in hip joint mechanics. *J Biomech* 36:171–178
31. Ferguson SJ, Bryant JT, Ganz R, Ito K (2000) The influence of the acetabular labrum on hip joint cartilage consolidation: a poroelastic finite element model. *J Biomech* 33:953–960
32. Ferguson SJ, Bryant JT, Ganz R, Ito K (2000) The acetabular labrum seal: a poroelastic finite element model. *Clin Biomech (Bristol, Avon)* 15:463–468
33. Jo WL, Lee WS, Chae DS, Yang IH, Lee KM, Koo KH (2016) Decreased lumbar lordosis and deficient acetabular coverage are risk factors for subchondral insufficiency fracture. *J Korean Med Sci* 31:1650–1655. <https://doi.org/10.3346/jkms.2016.31.10.1650>
34. Nicayenzi B, Shah S, Schemitsch EH, Bougherara H, Zdero R (2011) The biomechanical effect of changes in cancellous bone density on synthetic femur behavior. *Proc Inst Mech Eng H* 225:1050–1060
35. Smith SD, Jansson KS, Philippon MJ, LaPrade RF, Wijdicks CA (2014) Fracture mechanics of the femoral neck in a composite bone model: effects of platen geometry. *J Biomech* 47:602–606. <https://doi.org/10.1016/j.jbiomech.2013.10.042>
36. Basso T, Klaksvik J, Syversen U, Foss OA (2014) A biomechanical comparison of composite femurs and cadaver femurs used in experiments on operated hip fractures. *J Biomech* 47:3898–3902. <https://doi.org/10.1016/j.jbiomech.2014.10.025>
37. Nakano N, Yip G, Khanduja V (2017) Current concepts in the diagnosis and management of extra-articular hip impingement syndromes. *Int Orthop* 41:1321–1328. <https://doi.org/10.1007/s00264-017-3431-4>